Colloids and Surfaces A: Physicochem. Eng. Aspects 497 (2016) 336–343

Contents lists available at ScienceDirect

Colloids and Surfaces A: Physicochemical and Engineering Aspects

journal homepage: www.elsevier.com/locate/colsurfa

Microscale liquid-liquid displacement dynamics: Molecular kinetic or hydrodynamic control

Bauyrzhan K. Primkulov[a,1], Feng Lin[b,1], Zhenghe Xu[a,c,*]

[a] Department of Chemical and Materials Engineering, University of Alberta, Edmonton, Alberta T6G 1H9, Canada
[b] CANMET Energy Technology Centre-Devon, Natural Resources Canada, One Oil Patch Drive, Devon, Alberta T9G 1A8, Canada
[c] Institute of Nuclear and New Energy Technology, Tsinghua University, Beijing 100084, China

HIGHLIGHTS

- Measurement of microscale oil-water wetting dynamics on a solid microsphere by micropipette technique.
- Strong dependence of wetting rates on interfacial properties over wide capillary numbers ca.
- Dominant role of molecular friction at low ca while increasing role of viscous dissipation at high ca.
- Proportional increase of contact line friction ζ with viscosity of wetting liquid μ.
- Strong dependence of molecular jump frequency k^0 and length λ on solid wettability.

GRAPHICAL ABSTRACT

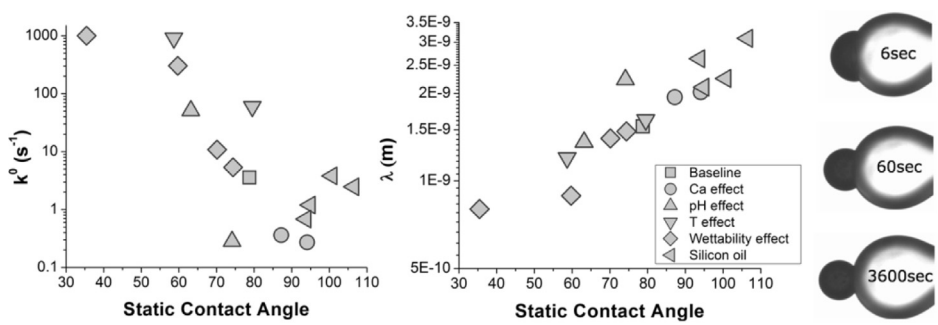

ARTICLE INFO

Article history:
Received 30 November 2015
Received in revised form 1 February 2016
Accepted 7 February 2016
Available online 2 March 2016

Keywords:
Wetting dynamics
Dynamic contact angle
Micropipette
Molecular kinetic model
Hydrodynamic dissipation model

ABSTRACT

Dynamic evolution of liquid/liquid/solid contact line at micrometer length scale, corresponding to the Bond number Bo∼0, was investigated in a system with tuneable interfacial properties. Viscous oil was spontaneously displaced by water on a micron size spherical glass surface. By controlling wettability of the substrate and chemistry of surrounding aqueous solution, the displacement dynamics of three phase contact lines over a wide range of capillary numbers were studied. The rates of spontaneous oil displacement showed a strong dependence on fluid viscosity and interfacial properties of the system. The observed wetting dynamics were modeled using hydrodynamic and molecular-kinetic theory. Energy dissipation in the immediate neighborhood of the contact line was shown to determine the wetting dynamics of our micron scale experiments, even when capillary numbers were well above 10^{-4} in which hydrodynamic flow regime could be usually expected for conventional macroscopic systems.

1. Introduction

Many industrial processes and life sciences involve liquid-liquid displacement from solid surfaces. This includes cleaning detergency, mineral flotation, bitumen extraction and fluid flow in microfluidics encountered in life science, material fabrication and enhanced oil recovery [1–3]. Here, one liquid displaces

* Corresponding author.
E-mail address: zhenghe@ualberta.ca (Z. Xu).
[1] B. K. Primkulov and F. Lin contributed equally to this work.

http://dx.doi.org/10.1016/j.colsurfa.2016.02.013
0927-7757/

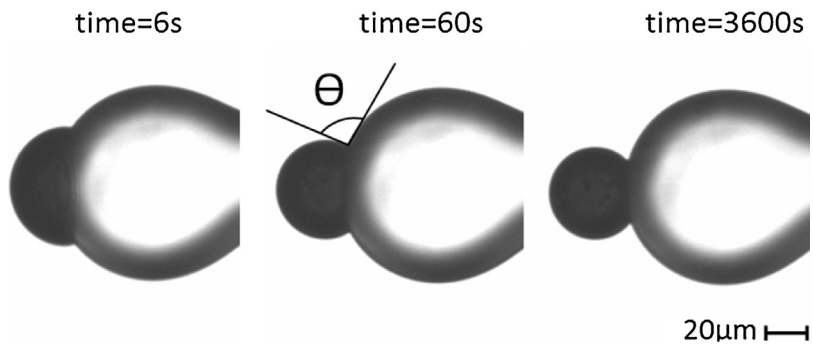

Fig. 1. Typical images showing oil displacement by water from a solid microsphere. The apparent contact angle θ is measured from the aqueous phase.

another until an optimal configuration is reached, which is normally described by contact angle of liquid-liquid interface on a solid surface. The process is often aided with the addition of chemicals, which modify interfacial properties of the system. Thus, in order to provide scientific directions to design systems that optimize conditions for relevant practical applications, understanding the mechanisms of liquid-liquid displacement and the parameters that control the rate of displacement can be crucial.

The majority of previous work in wetting dynamics focused on liquid/gas/solid systems. A typical example would be the spreading of a liquid drop of several millimeters in size on a smooth, homogeneous, flat surface in air. To describe the underlying physics behind the process, either molecular-kinetic or hydrodynamic approach, which differ mostly in consideration of dominant energy dissipation mechanisms, are largely adopted. Both models are widely applied to describing numerous liquid-gas experiments, and several thorough reviews [4–6] are available. In contrast, liquid-liquid displacement has been investigated sparsely, and even less so for the droplet recession on the micrometer sized solid surfaces, despite its great scientific and practical importance.

Some of the early liquid-liquid displacement experiments were analyzed using hydrodynamic approach. Foister [7] investigated spontaneous displacement of one liquid by another from smooth and flat solid surfaces. Immiscible liquids of wide viscosity range were used. The viscosity ratio was found to have a significant effect on the rate of displacement. Foister tied the experimental observations with hydrodynamic theory of Cox [8], where liquid viscosity ratio plays a critical role. Essentially hydrodynamic approach assumes that three-phase contact line is driven by capillary forces while excess energy is lost through viscous dissipation in either liquid. However, Fermigier and Jenffer [9] pointed out that purely hydrodynamic model systematically underestimates dynamic contact angles when carefully compared with the experimental results. In fact, Sheng and Zhou [10] suggested another dissipation mechanism that might play an important role, especially for the systems below certain capillary number range.

At low capillary numbers, viscous dissipation in liquid bulk becomes negligible and contact line displacement rate is controlled by adsorption/desorption processes described in molecular-kinetic theory of Blake and Haynes [11]. This approach suggests that majority of energy dissipation takes place in immediate vicinity of contact line, and the displacement rate depends on the nature of liquid-solid interactions. Ramiasa et al. [12] investigated slow displacement of water by millimeter size dodecane droplets from the flat thiol-coated gold surfaces. Immiscible liquid phases in their study were kept constant, while substrate wettability was altered by applying varying degrees of thiol coating. Ramiasa et al. were able to demonstrate experimentally that whenever molecular-kinetic approach was applicable, wetting line energy dissipation changed exponentially with work of adhesion.

Fetzer et al. [13] suggested that it is possible to decide based on capillary number range whether molecular-kinetic or hydrodynamic mechanisms control the rate of wetting line displacement. The authors established that molecular-kinetic approach describes liquid-liquid displacement from solid surfaces very well, as long as associated capillary numbers are below 2×10^{-4}. In the range of capillary numbers above 2×10^{-4}, Fetzer et al. recommended hydrodynamic models although unrealistic fitting parameters were produced. The discrepancy was explained by possible inertial deterioration of contact line displacement at high displacement rates. It should be emphasized that majority of existing studies on liquid-liquid displacement dynamics, as described above, are limited to the so-called macroscopic systems where flat solid substrates and liquid droplets with over 1 mm in size are usually used. Most recently, Lin et al. [14] (our research group) investigated dynamic dewetting of a solid microsphere by individual emulsion liquid droplets, where inertial effects could be safely neglected. It was found that in certain cases both molecular-kinetic and hydrodynamics based models produce good fit to the experimental data. This finding suggests that there might be a range of experimental conditions where both adsorption/desorption mechanisms and hydrodynamic dissipation in liquid bulk have a comparable impact on liquid-liquid displacement rates.

In this communication, we report the reverse process,—spontaneous wetting of an immiscible viscous oil droplet by water from micron size spherical glass surfaces (Fig. 1). System parameters that include surface treatment of solid, characteristics of oil, water chemistry (pH and electrolyte concentration), and temperature were tuned to investigate their effects on the microscale displacement dynamics of liquid-liquid wetting line. This system is of special interest, since the associated gravitational and inertial effects are negligibly small (Bond number less than 10^{-5}, Weber number less than 10^{-10}) and the distortion of liquid droplet profile at the three-phase contact line could be therefore ruled out. Most importantly, by controlling the system's important physicochemical properties including solid wettability, interfacial tension, and viscosity of immiscible liquids, capillary numbers of the system can be varied widely as desired. As a result, we are able to examine how well the available models describe microscale three-phase contact line displacement dynamics over a wide range of capillary numbers. Molecular-kinetic model was found to fit experimental data at capillary numbers well above 10^{-4}, which is a cross over region between thermally activated and hydrodynamic flow regimes suggested in literature [6,13].

2. Materials and methods

The present experiments were performed using a setup modified to what we reported previously [14], where detailed description on fabrication of micro-spherical tips was given.

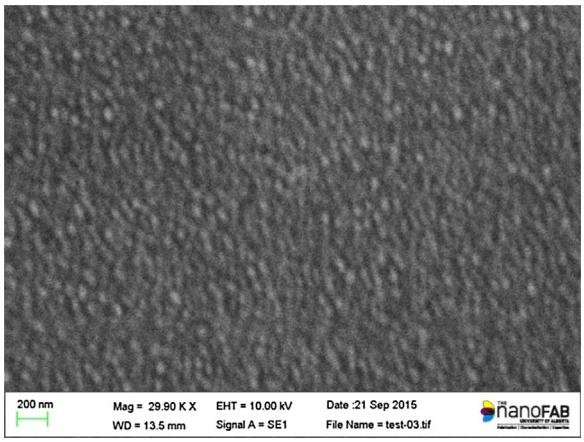

Fig. 2. Scanning electron microscope image of freshly fabricated micron size spherical glass surface. The root-mean-square surface roughness was determined to be 1 nm. The nanometer scale features in the image were due to the pre-coated gold film of nanometer thickness on sputtering tool, required to obtain high quality SEM images.

However, oil displacement experiments were carried out in this study as follows: first each micron size solid surface was coated with a thin meniscus of viscous oil in air, and then immersed in aqueous electrolyte solutions of controlled pH and ion concentration at a given temperature. Spontaneous relaxation of oil droplet as water advanced on solid surface was monitored using an optical microscope (Zeiss Axiovert 200). The resulting images (Fig. 1) were analyzed to obtain the temporal evolution of water advancing contact angle, i.e., the angle between two tangent lines drawn at three-phase contact point measured from the aqueous phase. A video clip demonstrating the displacement process is given in the supporting information.

Any real surface has a degree of heterogeneity associated with it, and it was our goal to reduce the scale of roughness on our substrates. Atomic scale smoothness is characteristic for liquid surfaces [15], and thus by solidifying molten glass in a clean environment one can produce very smooth substrates. This phenomenon is in fact utilized in a production of floated glass, where glass flows on liquid tin surface and liquid-like smooth substrates are generated [15].

Much like floated glass fabrication process, our micron size spherical glass substrates were melted next to hot platinum wires and allowed to solidify in clean laboratory environment. The root-mean-square surface roughness of our glass substrate was found to be about 1 nm, as illustrated by the image of scanning electron microscope in Fig. 2. The surface can be considered smooth (note that it was essential to coat a nanometer scale layer of gold for scanning electron microscope imaging of our non-conducting substrates, with the nanometer scale features in Fig. 2 being likely produced by gold sputtering).

Effects of solution pH and $CaCl_2$ concentration on viscous oil relaxation were examined on freshly fabricated micron size spherical tips at room temperature. Aqueous solutions were prepared from deionized water, to which certain amounts of salts were added. A baseline solution contained 100 ppm of $NaHCO_3$ and 500 ppm of NaCl, with pH being controlled at 8.0 by the addition of NaOH. This solution was further modified by either adding $CaCl_2$ or increasing pH (Table 1). Viscous oil used in this study was coker-feed bitumen (CFB) provided by Syncrude Canada. The viscosity (μ) of bitumen changes exponentially with temperature, which was measured using a rotational rheometer (TA Instruments AR-G2). In contrast, the change in bitumen-water interfacial tension (γ) could be considered negligible if there is any over the temperature ranges studied [16–23]. Instead, the significant change of bitumen-water interfacial tensions could be readily achieved through the change of aqueous electrolyte ion concentration and pH [16,17,20,21,24–27], which was measured using emulsion drop-shape recovery technique developed by Moran et al. [24]. In this novel technique, the bitumen-aqueous phase interfacial tension was determined from characteristic time of shape recovery of elongated emulsion drops, with the known fluid viscosity of the droplets determined independently using the above-mentioned rheometer.

As shown in Table 1, the trends and magnitudes of the measured interfacial tension in alkaline solutions (pH 8–11) at ambient conditions in this study were consistent with those reported previously on bitumen from Athabasca oil sands [16,17,20,24–26] and Utah tar sands [21,27]. Silicon oils (SO) with a range of viscosities (denoted as s12 to s97) measured by the AR-G2 rheometer and interfacial tensions measured by a conventional Kruss K-12 process tensiometer were also used in a few control tests. Due to their great difficulties for direct measurements and very slight impact of temperature, bitumen-water interfacial tensions at higher temperatures (50 °C and 70 °C) were estimated via linear extrapolation using a temperature coefficient of −0.013 mN/(m· deg) as suggested by Drelich [16].

Effect of solid wettability on three phase contact line displacement velocity was investigated by controlling the affinity of micron size glass surface to water. This was achieved by controlled hydrolysis of the freshly prepared micron size spherical glass tips immersed in the baseline aqueous solution for a period of time prior to oil coating and displacement experiments. The longer the glass tip was exposed to water, the higher its affinity to aqueous phase and hence the water wettability.

In each of the displacement experiments, the dynamic water-advancing contact angle was observed to reduce rapidly at early stages and the change slowed down when it is approaching a static (constant) value. Wetting line displacement velocity showed a strong dependence on surface wettability of the micron size sphere, chemistry of aqueous solution and viscosity of oil. By adjusting these parameters we were able to cover a wide range of capillary numbers, and thus test applicability of hydrodynamic and molecular-kinetic models to liquid-liquid displacement dynamics from solid surfaces.

3. Dynamic displacement models

Hydrodynamic (HD) model of wetting line displacement typically involves solving creeping flow equation in the vicinity of the contact line. Huh and Scriven [28] were among the first to take this approach when investigating flow near simple wetting line wedge. Taking a conventional no-slip boundary condition between a liquid and a solid, they found that hydrodynamic solution results in unbounded stresses at the wetting line [28]. This unbounded stress is a common problem to all hydrodynamic solutions of dynamic wetting, and it is normally attributed to rheological anomalies and breakdown of the continuum assumption at the contact line. One way around this problem is to relax no-slip boundary condition in the immediate neighborhood of the wetting line; hence a typical hydrodynamic solution would include a phenomenological slip-length parameter L_m.

One of the most complete hydrodynamic solutions of liquid-liquid displacement on the solid surface was developed by Cox [8,29]. In his model, wetting line neighborhood was divided into inner, intermediate and outer regions, and the matched asymptotic expansions were used to link apparent contact angle with the wetting line displacement velocity. We should note that in our system, oil viscosity is many orders of magnitude greater than viscosity of water, and viscous dissipation dominantly occurs in the core of oil

Table 1
Viscosities (μ) of viscous oils and oil-water interfacial tensions (γ) of systems used in displacement tests.

Denote	Oil	$CaCl_2$ (ppm)	pH	γ (mN/m)	μ (Pa·s)
baseline	CFB	0	8.0	13.9#	1040.0
Ca100	CFB	100	8.0	14.3#	1040.0
Ca200	CFB	200	8.0	15.2#	1040.0
pH10	CFB	0	10.0	7.9#	1040.0
pH11	CFB	0	11.0	4.9#	1040.0
T50	CFB	0	8.0	13.6$	66.7
T70	CFB	0	8.0	13.3$	8.5
s12	SO12	0	8.0	44.0‖	12.2
s29	SO29	0	8.0	38.0‖	29.2
s58	SO58	0	8.0	40.6‖	58.4
s97	SO97	0	8.0	30.8‖	97.3

#Measured by drop-shape recovery method.
$Estimated by linear extrapolation suggested by Drelich [16].
‖Measured by K12 process tensometer.

Table 2
Optimal fitting parameters of experimental results to hydrodynamic (HD) and molecular-kinetic (MK) models.

Denote	θ_S (deg)	L_m (m)	95% CI (m)	k^0 (s^{-1})	λ (nm)
baseline	79	5×10^{-47}	2×10^{-50}; 1×10^{-43}	3.6±0.3	1.54±0.01
wettability2	74	8×10^{-40}	9×10^{-43}; 7×10^{-37}	5.4±0.4	1.48±0.01
wettability3	70	2×10^{-28}	2×10^{-30}; 1×10^{-26}	11±1	1.40±0.01
wettability4	60	3×10^{-11}	2×10^{-11}; 5×10^{-11}	303±15	0.89±0.01
wettability5	35	7×10^{-09}	6×10^{-9}; 9×10^{-9}	1000±245	0.80±0.05
pH10	74	3×10^{-91}	1×10^{-98}; 8×10^{-84}	0.28±0.2	2.23±0.01
pH11	63	5×10^{-15}	2×10^{-15}; 1×10^{-14}	51±7	1.36±0.05
Ca100	87	6×10^{-110}	2×10^{-121}; 2×10^{-98}	0.36±0.2	1.94±0.01
Ca 200	94	2×10^{-99}	8×10^{-110}; 5×10^{-89}	0.27±0.2	2.02±0.01
T50	80	2×10^{-40}	1×10^{-42}; 3×10^{-38}	60±3	1.62±0.01
T70	59	2×10^{-129}	1×10^{-135}; 2×10^{-123}	912±94	1.20±0.03
s12	95	2×10^{-222}	3×10^{-246}; 1×10^{-198}	1.2±0.6	2.10±0.07
s29	94	3×10^{-183}	4×10^{-218}; 2×10^{-148}	0.7±0.2	2.63±0.06
s58	101	2×10^{-87}	3×10^{-105}; 1×10^{-69}	3.8±0.3	2.25±0.02
s97	106	3×10^{-32}	5×10^{-37}; 3×10^{-27}	2.5±0.2	3.09±0.03

droplet rather than in water. Thus, Cox's solution takes its simplest form, resulting in the following governing equation [5].

$$U = \frac{\gamma\left[\pi - \theta_S{}^3 - \pi - \theta^3\right]}{9\mu \ln L/L_m}, \; for\, \theta > \pi/4 \quad (1)$$

where U is the wetting line displacement velocity, θ is the dynamic water-advancing contact angle with (π−θ) being the dynamic contact angle measured from oil phase, θ_S is the static contact angle, γ and μ are oil-water interfacial tension and viscosity of oil, respectively, L and L_m

are macroscopic and microscopic length scales of the system. Essentially, in hydrodynamic solution, capillary forces drive the droplet toward the equilibrium shape while viscous dissipation in the droplet bulk retards the wetting line displacement. It is important to note that microscopic length scale L_m is not known a priory, and it is often used as a fitting parameter to experimental observations. This slip length is not expected to be smaller than molecular length scale [4], and thus applications with smaller fitted values of L_m could be governed by other mechanisms.

Molecular-kinetic (MK) approach [11] suggests that wetting rate can be controlled by adsorption-desorption processes at the wetting line on the solid. It assumes that solid surface has a large number of identical adsorption sites. Liquid molecules can attach to or detach from these sites, and there are energy barriers associated with this process. In the case of oil droplet displacement, the difference between the static and dynamic contact angles alters corresponding energy barriers. The new energy barrier makes water adsorption to glass more favorable, forcing the oil to recede from the solid surface. Molecular-kinetic solution involves two key parameters: typical distance between adsorption sites λ, and frequency k° of adsorption/desorption events at equilibrium. The relationship for the wetting line velocity is given by

$$U = 2k^0\lambda\sinh\left(\frac{\gamma\left[\cos\left(\pi-\theta\right)-\cos\left(\pi-\theta_S\right)\right]\lambda^2}{2k_BT}\right), \quad (2)$$

where k_B is the Boltzmann constant, and T is the absolute temperature. Typical distance between adsorption sites λ, and frequency of adsorption/desorption events k° are normally used as fitting parameters. These two parameters can be combined into a coefficient of wetting line friction $\left(\zeta = \frac{k_BT}{k^0\lambda^3}\right)$, which is a measure of energy losses due to molecular processes at the contact line. In molecular-kinetic theory, energy is dissipated at the contact line, and viscous dissipation in liquid bulk is considered negligible.

Fitting parameters are inevitable in both models of dynamic displacement. In hydrodynamic solution of wetting/dewetting, parameter L_m is often referred to as cutoff or slip length, and it is a necessary tool for removing the unbounded stresses at the contact line.

At the same time it is not well understood how the value of the slip length depends on the physical properties of the system. de Gennes suggested that the slip length of a fluid flowing over a smooth solid surface should be comparable to a the scale of molecules [4]. However when the flowing fluid is a polymer melt, the values of the slip length can be significantly greater than the nanometer scale [4]. Similarly, there is no definitive way to predict the values of molecular kinetic parameters λ and k°. While λ is expected to be of molecular scale, the frequency of displacement events k° is known to vary greatly [5].

As a result, theoretical models of displacement dynamics are normally fit to the experimental data using k° and λ or L_m as fitting parameters [5,12,13,20,30]. In our work we optimized the values of either L_m (HD model), or k° and λ (MK model) to produce the best fit to experimental curves with least square errors. The fitting was done by utilizing bounded trust region approach [31,32] with maximum number of function evaluations set to 5000 and abscissa and ordinate tolerances set to 10^{-30}. Estimates of 95 percent confidence intervals were obtained for each fitting parameter from the residuals and the Jacobian of nonlinear fitting.

The fundamental difference between the two models is the source of energy dissipation. While hydrodynamic model assumes that the excess energy is lost due to viscous dissipation in liquid bulk, molecular-kinetic model assumes that energy is dissipated in the immediate neighborhood of the contact line.

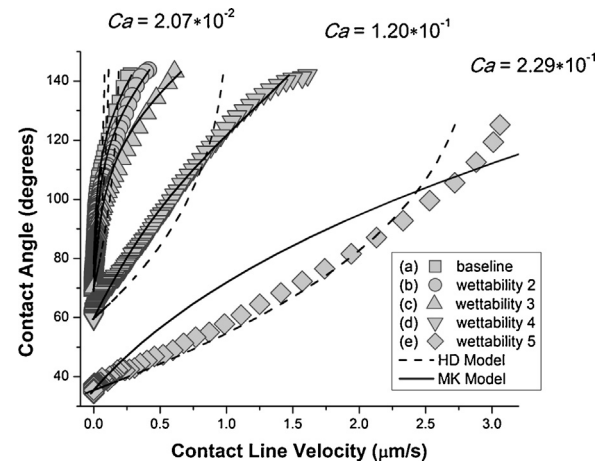

Fig. 3. Effect of micron size spherical glass wettability on liquid-liquid displacement velocity at ambient temperature. See Table 2 for fitting parameter values.

4. Results and discussion

4.1. Effect of solid wettability

Wetting line velocity exhibited a strong dependence on substrate wettability: oil droplets receded faster on more hydrophilic surfaces. Fig. 3 shows the faster contact angle evolution with increasing the degree of substrate hydrophilicity from (a) to (e). Since the chemistry and temperature of water and oil phases were kept constant from one experiment to another, the only factor that changed was the strength of solid-liquid interactions at the contact line.

Theoretical fitting of the experimental data with hydrodynamic model (Eq. (1)) generates unrealistically small values of the slip length L_m for curves (a) to (d) in Fig. 3. All of these experiments have associated capillary numbers below 0.12. On the other hand, the fit of the hydrodynamic model is improved for curve (e), where parameter L_m is of nanometer scale. Fig. 3 also displays the molecular-kinetic curve fitting to wettability data. While parameter λ remains within the nanometer scale for all the experiments, the frequency parameter k° increases sharply from (a) to (e). Since the only condition that changed from one experiment to another was the substrate wettability, we find that the frequency of adsorption/desorption events at equilibrium k° strongly depends on the strength of solid-liquid interactions.

Overall, we observe a qualitative transition from molecular-kinetic model to hydrodynamic model as the capillary number increases. While molecular-kinetic model produces a good fit to the experiments with capillary numbers below 0.12, hydrodynamic curve has a closer fit to experiment (e) in Fig. 3.

4.2. Effect of pH

It is believed that changes in aqueous solution pH affect both oil-water and glass-water interfaces. Higher pH values aid ionization and accumulation of natural surfactants at oil-water interface [33]. This reduces oil-water interfacial tension γ, which was verified with our drop shape recovery tests (Table 1). At the same time, increased concentration of the OH^- group in aqueous solution also triggers higher degree of deprotonation of hydrolyzed substrate surface [33]. The glass surface accumulates additional negative charges [33], which makes the surface more hydrophilic [34].

As illustrated in Fig. S1, the initial displacement rates of viscous oil from the untreated glass microsphere in ambient aqueous

solutions decreased from (a) to (b), and then increased from (b) to (c) as solution pH increased from 8.0 to 10.0, and 11.0. At a higher aqueous pH, the glass surface becomes more hydrophilic, and thus oil should be displaced faster from the glass surface. However, higher values of pH also reduce oil-water interfacial tension (Table 1). Smaller values of γ reduce the numerators in governing equations of hydrodynamic and molecular-kinetic models (see Eqs. (1)–(2)), and hence reduce the driving force for the displacement of three phase contact line. As a result, there is a competing effect between the more hydrophilic substrate and smaller driving force for oil displacement as the aqueous solution pH increases from 8.0 to 11.0. Results in Fig. S1 demonstrate a closer fit to molecular kinetic model, while hydrodynamic fitting produces L_m parameter well below the scale of molecules. This finding suggests that the oil displacement in above experiments is governed by energy dissipation mechanisms at the contact line rather than hydrodynamic viscous dissipation in the liquid bulk.

4.3. Effect of $CaCl_2$

Much like the effect of solution pH, the presence of Ca^{2+} ions modifies both oil-water and glass-water interfaces. Compared with the effect of pH, however, the changes are in the opposite direction. Ca^{2+} ions reduce the concentration of natural surfactant at the oil-water interface [33], and thus slightly increase oil-water interfacial tension, as shown in our interfacial tension measurements (Table 1). Moreover, at solution pH of 8.0 and above, calcium monohydroxy ions ($CaOH^+$) adsorb on hydrolyzed silica surfaces (SiO^-) forming covalent SiOCa linkage, which reduces the overall negative charge of the substrate [33,35]. As a result, the glass surface becomes less hydrophilic.

Fig. S2 shows experimental displacement velocity profiles on the untreated solid surface in ambient aqueous solutions of different $CaCl_2$ concentrations. As the concentrations of the divalent salt increased from (a) to (c), the corresponding oil displacement rates decreased. The experimental results of the displacement dynamics at different $CaCl_2$ concentrations are closely matched by molecular-kinetic model. The frequency parameter k° is smaller on less hydrophilic substrate surfaces, while λ remains within the nanometer length scale.

4.4. Effect of viscosity

In aforementioned experiments, the system's interfacial properties were modified and oil viscosities were kept constant. However, reducing the liquid viscosity can be another powerful tool to aid oil displacement. In our experiments oil viscosity was reduced exponentially with increasing its temperature.

Fig. S3 shows the temporal contact angles of oil droplets at 25 °C, 50 °C, and 70 °C. It is interesting to note from Fig. S3 a close fit of experimental data by molecular-kinetic model. Parameter k° increases for experiments with less viscous oil, which confirms the inverse relation between k° and fluid viscosity, as suggested by Blake [5].

It is important to note that when the silica surface is not fully hydrolyzed, which was the case in our micropipette experiments, high temperature of aqueous phase could accelerate hydrolysis and deprotonation of the substrate. As a result, the solid surface would become more hydrophilic, and static contact angle would decrease, which was observed in our droplet displacement experiments at 70 °C.

The above set of experiments was supplemented with the tests using pure silicon oils with the results shown in Fig. S4. In this case, natural surfactants were not present in silicon oil and in the system, which resulted in higher oil-water interfacial tensions (see Table 1). Silicon oils had a range of viscosities, and their displacement velocity profiles were more closely matched by molecular-kinetic rather than by hydrodynamic model.

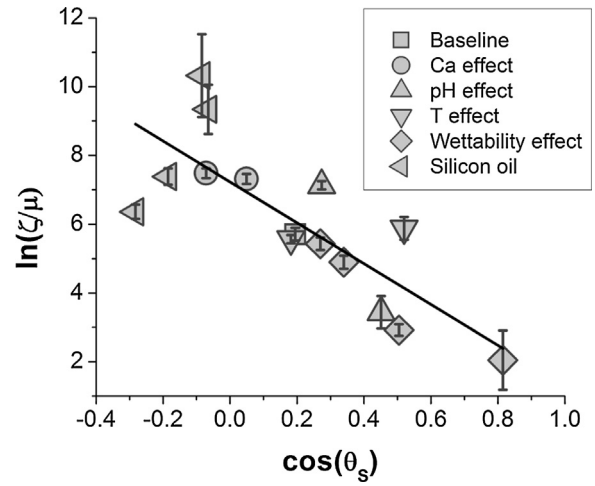

Fig. 4. Relation between the normalized wetting line friction coefficient and cosine of the static contact angle.

4.5. Discussion on wetting line friction

Overall, we observed strong dependence of the rates of spontaneous liquid-liquid displacement on the final (static) contact angle in all of our experiments. In fact, Blake and Coninck proposed based on a group of experimental studies that the wetting line friction coefficient depends linearly on viscosity and exponentially on work of adhesion, a measure of energy needed to separate oil from the substrate immersed in an aqueous phase, as shown in Eq. (3) [36]:

$$\zeta \approx \frac{\mu v_L}{\lambda^3} \exp\left(\frac{W_a \lambda^2}{k_B T}\right), \tag{3}$$

where v_L is volume of flow unit, and W_a equals $\gamma(1-\cos\theta_S)$. The above equation can be rearranged to become $\ln\left(\frac{\zeta}{\mu}\right) \approx \ln\left(\frac{v_L}{\lambda^3}\right) + \frac{\gamma\lambda^2}{k_B T} - \frac{\gamma\lambda^2}{k_B T}\cos\theta_S$. Hence, in a system where molecular-kinetic description of wetting applies, plotting experimental values of $\ln(\zeta/\mu)$ versus $\cos\theta_S$ leads to a straight line.

Molecular-kinetic fitting parameters k° and λ are combined into the wetting line friction coefficients, and $\ln(\zeta/\mu)$ is plotted against cosine of static contact angle (θ_S) in Fig. 4. The wetting line friction coefficient has the same units as the fluid viscosity and can be used as a measure of resistance to flow at the contact line. From the slope of the straight line in Fig. 4, we can deduce that the molecular jump length λ is about 1.12 nm (see Eq. (3)). It appears that the jump length λ remains close to the calculated value in each case where the MK model is applicable to our systems. A typical flow volume v_L in our set of experiments can be obtained from a known value of λ and the intercept value in Fig. 4, and it is estimated to be 5.1 nm^3. These two parameter values are in a good agreement with the molecular nature of the MK model [5]. Most importantly, Fig. 4 shows that the wetting line friction ζ for our two-liquid systems increases in proportion with viscosity of the wetting liquid μ, and it increases exponentially with increasing system's static contact angle, as predicted. It is also worth noting that although the jump length λ appears nearly unaffected by the viscosity, the jump frequency k° varies inversely with the viscosity, since ζ has a linear relation to μ. Therefore, lower viscosity results in a lower value of the friction coefficient and hence higher frequency. Our results of the solid/liquid/liquid displacement provide further evidence that whenever viscous interactions with neighboring fluid molecules remain significant in the wetting

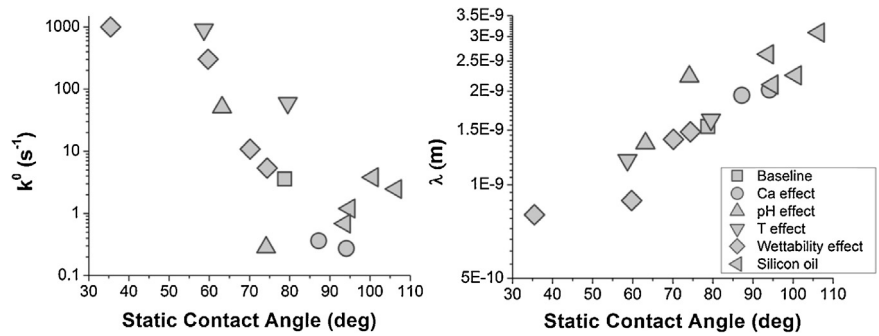

Fig. 5. Correlation of molecular-kinetic model fitting parameters to substrate wettability.

line friction and interfacial destruction/creation process, molecular adsorption/desorption at contact line may be the underlying mechanism of dynamic wetting. It is reinforced from our results that both viscosity and interfacial tension are critical physicochemical parameters in the molecular kinetic theory [14,36,37].

4.6. Surface heterogeneity

Alternatively, adsorption/desorption events (molecular jumps) of the molecular-kinetic model can be viewed as a stick-slip propagation of the interface on a substrate with small surface heterogeneities [6]. Therefore, the wetting line friction coefficient can be interpreted as dissipation at the contact line due to energy barriers associated with surface imperfections. In fact, molecular-kinetic equation of wetting is found to provide effective description on contact line displacement in the presence of surface imperfections [6]. In this case λ and k° represent the length scale and frequency of stick/slip events. Hence, one can expect that the length λ of these stick/slip events is similar in scale to surface heterogeneities. In fact, parameter λ remains in the range of few nanometers in all of our displacement experiments (Fig. 5), which is consistent with the estimates the scales of our system's surface heterogeneity features (Fig. 2). It is interesting to note that both λ and k° vary with the degree of solid wettability (static contact angle) in Fig. 5. This dependence means that the scale and the frequency of the stick/slip events are correlated to the variations in the substrate nanoscale wettability. In other words, changes in substrate wettability can be responsible for altering the scale of surface imperfections or energy barriers associated with the stick/slip events.

In search for an alternative explanation on our dynamic wetting characteristics, we fitted our experimental results to hydrophilic/hydrophobic lattice (HHAL) model developed by Liu et al. to quantify specifically the surface dynamic behavior of polymers [38]. As shown in Fig. S5 given in the supplementary information, the model fitted very well with our experimental results. However the fitted model parameters given in Table S1 of the supplementary information were orders of magnitude different from the values presented by Liu, et al. This is not surprising as our substrate is not a polymer. In our case, the contact line displacement dynamics are not governed by diffusional migrations of hydrophobic moieties from substrate to liquid bulk. This is because the glass substrate in our study is hydrophilic throughout the dynamic displacement process of oil droplet as a result of spreading a layer of viscous oil on hydrophilic glass surfaces. In our case, the displacement of the contact line is driven toward equilibrium shape by uncompensated interfacial forces ($F = \gamma\left[\cos\left(\pi - \theta\right) - \cos\left(\pi - \theta_S\right)\right]$).

5. Conclusions

Overall, this work presents an important advance in providing experimental data and physical outlook of micron scale liquid-liquid displacement on solid surfaces over a wide range of capillary numbers in the absence of gravity and inertial effects. It has been demonstrated that at micron scale both viscosity and interfacial properties of the system can be used to adjust the rates of spontaneous liquid-liquid displacement. The rates of liquid-liquid displacement were defined by energy dissipation mechanisms in the immediate vicinity of contact line at low capillary numbers, while viscous dissipation defined dynamic wetting of higher capillary numbers. In our experiments, the qualitative transition from one model to another did not take place at 10^{-4}, but occurred at higher values of capillary number. This finding suggests that even nanometer scale surface heterogeneities can significantly shift the cross-over region between the hydrodynamic and wetting line friction dominated flows in micron scale droplets.

Acknowledgements

The financial support for this work provided by the Natural Science and Engineering Research Council of Canada under the Industrial Research Chair Program in Oil Sands Engineering and Alberta Innovates-Energy and Environmental Solutions is gratefully acknowledged. The partial support (ZXU) by the National Science Foundation of China (grant number 21333005) for this work is also acknowledged.

Appendix A. Supplementary data

Supplementary data associated with this article can be found, in the online version, at http://dx.doi.org/10.1016/j.colsurfa.2016.02.013.

References

[1] E. Bertrand, T.D. Blake, J. De Coninck, Dynamics of dewetting, Colloids Surf. A: Physicochem. Eng. Aspects 369 (2010) 141–147.
[2] Y.C. Jung, B. Bhushan, Wetting behavior of water and oil droplets in three-phase Interfaces for hydrophobicity/philicity and oleophobicity/philicity, Langmuir 25 (2009) 14165–14173.
[3] S. Basu, K. Nandakumar, J.H. Masliyah, Effect of NaCl and MIBC/kerosene on bitumen displacement by water on a glass surface, Colloids Surf. A: Physicochem. Eng. Aspects 136 (1998) 71–80.
[4] P.G. de Gennes, Wetting: statics and dynamics, Rev. Mod. Phys. 57 (1985) 827–862.
[5] T.D. Blake, The physics of moving wetting lines, J. Colloids Interface Sci. 299 (2006) 1–13.
[6] J.H. Snoeijer, B. Andreotti, Moving contact lines: scales, regimes, and dynamical transitions, Annu. Rev. Fluid Mech. 45 (2013) 269–292.
[7] R.T. Foister, The kinetics of displacement wetting in liquid/liquid/solid systems, J. Colloids Interface Sci. 136 (1990) 266–282.
[8] R. Cox, The dynamics of the spreading of liquids on a solid surface. Part 1. viscous flow, J. Fluid Mech. 168 (1986) 169–194.

[9] M. Fermigier, P. Jenffer, An experimental investigation of the dynamic contact angle in liquid-liquid systems, J. Colloids Interface Sci. 146 (1991) 226–241.
[10] P. Sheng, M. Zhou, Immiscible-fluid displacement: contact-line dynamics and the velocity-dependent capillary pressure, Phys. Rev. A 45 (1992) 5694–5708.
[11] T. Blake, J. Haynes, Kinetics of liquid-liquid displacement, J. Colloids Interface Sci. 30 (1969) 421–423.
[12] M. Ramiasa, J. Ralston, R. Fetzer, R. Sedev, Contact line friction in liquid-liquid displacement on hydrophobic surfaces, J. Phys. Chem. C 115 (2011) 24975–24986.
[13] R. Fetzer, M. Ramiasa, J. Ralston, Dynamics of liquid-liquid displacement, Langmuir 25 (2009) 8069–8074.
[14] F. Lin, L. He, B. Primkulov, Z. Xu, Dewetting dynamics of a solid microsphere by emulsion drops, J. Phys. Chem. C 118 (2014) 13552–13562.
[15] P.G. De Gennes, F. Brochard-Wyart, D. Quéré, Capillarity and Wetting Phenomena: Drops Bubbles Pearls Waves, Springer Science Business Media, 2013.
[16] J. Drelich, The role of wetting phenomena in the hot water process for bitumen recovery from tar sand, PhD dissertation, university of utah, salt lake city Utah 1993.
[17] E.E. Isaacs, K.F. Smolek, Interfacial tension behaviour of Athabasca bitumen/aqueous surfactant systems, Can. J. Chem. Eng. 61 (1983) 233–240.
[18] J. Long, J. Drelich, Z. Xu, J.H. Masliyah, Effect of operating temperature on water-based oil sands processing, Can. J. Chem. Eng 85 (2007) 726–736.
[19] L.L. Schramm, E.N. Stasiuk, H. Yarranton, B.B. Maini, B. Shelfantook, Temperature effects from the conditioning and flotation of bitumen from oil sands in term of oil recovery and physical properties, J. Can. Petroleum Technol. 42 (2003) 55–61.
[20] S. Basu, K. Nandakumar, J.H. Masliyah, A study of oil displacement on model surfaces, J. Colloids Interface Sci. 182 (1996) 82–94.
[21] J. Drelich, J.D. Miller, Surface and interfacial tension of the Whiterocks bitumen and its relationship to bitumen release from tar sands during water processing, Fuel 73 (1994) 1504–1510.
[22] J. Masliyah, Z. Zhou, Z. Xu, J. Czarneck, H. Hamza, Understanding water-based bitumen extraction from Athabasca oil sands, Can. J. Chem. Eng. 82 (2004) 628–654.
[23] C.W. Bowman, Molecular and interfacial properties of Athabasca tar sands, in: Proc. of 7th World Petroleum Congress, Elsevier Publishing Co., Amsterdam, Netherlands, 1967, pp. 628–654.
[24] K. Moran, A. Yeung, J. Masliyah, Shape relaxation of an elongated viscous drop, J. Colloids Interface Sci. 267 (2003) 483–493.
[25] K. Takamura, E.E. Isaacs, Interfacial properties, in: L.G. Helper, C. Hsi (Eds.), AOSTRA Technical Handbook on Oil Sands, Bitumen and Heavy Oils, AOSTRA, Edmonton, Alberta, 1989, pp. 100–128.
[26] K. Moran, Role of interfacial properties on the stability of emulsified bitumen droplets, Langmuir 23 (2007) 4167–4177.
[27] J. Drelich, D. Lelinski, J. Hupka, J.D. Miller, The role of gas bubbles in bitumen release during oil sand digestion, Fuel 74 (1995) 1150–1155.
[28] C. Huh, L.E. Scriven, Hydrodynamic model of steady movement of a solid/liquid/fluid contact Line, J. Colloids Interface Sci. 35 (1971) 85–101.
[29] R. Cox, The dynamics of the spreading of liquids on a solid surface. Part 2. surfactants, J. Fluid Mech. 168 (1986) 195–220.
[30] M.J. De Ruijter, J. De Coninck, G. Oshanin, Droplet spreading: partial wetting regime revisited, Langmuir 15 (1999) 2209–2216.
[31] T. Coleman, Y. Li, An interior, trust region approach for nonlinear minimization subject to bounds, SIAM J. Optim. 6 (1996) 418–445.
[32] T. Coleman, Y. Li, On the convergence of reflective newton methods for large-scale nonlinear minimization subject to bounds, Math. Program 67 (1994) 189–224.
[33] J.H. Masliyah, J. Czarnecki, Z. Xu, Handbook on Theory and Practice of Bitumen Recovery from Athabasca Oil Sands, Kingsley Knowledge Publishing, 2011.
[34] J. Ralston, G. Newcombe, Static and dynamic contact angles, in: Developments in Mineral Processing, Elsevier, 1992.
[35] J. Liu, Z. Xu, J. Masliyah, Studies on bitumen-silica interaction in aqueous solutions by atomic force microscopy, Langmuir 19 (2003) 3911–3920.
[36] T. Blake, J.D. Coninck, The influence of solid-liquid interactions on dynamic wetting, Adv. Colloid Interface Sci. 96 (2002) 21–36.
[37] D. Duvivier, D. Seveno, R. Rioboo, T.D. Blake, J. De Coninck, Experimental evidence of the role of viscosity in the molecular kinetic theory of dynamic wetting, Langmuir 27 (2011) 13015–13021.
[38] F.P. Liu, D.J. Gardner, M.P. Wolcott, A model for the description of polymer surface dynamic behavior 1. contact angle vs polymer surface properties, Langmuir 11 (7) (1995) 2674–2681.